EUROPEAN ORGANIZATION FOR NUCLEAR RESEARCH

CERN-EP/99-131
September 27, 1999

Measurement of Triple-Gauge-Boson Couplings of the W Boson at LEP

The L3 Collaboration

Abstract

We report on measurements of the triple-gauge-boson couplings of the W boson in e^+e^- collisions with the L3 detector at LEP. W-pair, single-W and single-photon events are analysed in a data sample corresponding to a total luminosity of 76.7 pb^{-1} collected at centre-of-mass energies between 161 GeV and 183 GeV. CP-conserving as well as both C- and P-conserving triple-gauge-boson couplings are determined. The results, in good agreement with the Standard-Model expectations, confirm the existence of the self coupling among the electroweak gauge bosons and constrain its structure.

Submitted to *Phys. Lett. B*

1 Introduction

During the 1996 and 1997 data taking periods, the centre-of-mass energy, $\sqrt{s}$, of the e^+e^- collider LEP at CERN was increased from 161 GeV to 172 GeV and 183 GeV. These energies are well above the kinematic threshold of W-boson pair production, $e^+e^- \rightarrow W^+W^-$.

W-pair production, single-W production ($e^+e^- \rightarrow We\nu$) and single-photon production ($e^+e^- \rightarrow \nu\bar{\nu}\gamma$) all depend on the trilinear self couplings among the electroweak gauge bosons γ, W and Z [1]. The non-Abelian gauge structure of the electroweak theory implies the existence of the triple-gauge-boson vertices γWW and ZWW [2].

To lowest order within the Standard Model [2] (SM), three Feynman diagrams contribute to W-pair production, the s-channel γ and Z-boson exchange and the t-channel ν_e exchange. The s-channel diagrams contain the γWW and ZWW vertices. At present centre-of-mass energies, single-W production is sensitive to the electromagnetic gauge couplings only. The γWW vertex appears in one of the contributing t-channel Feynman diagrams in Weν production, and dominates the corresponding diagram containing the ZWW vertex. Radiation of a photon from the t-channel exchanged W boson in the process $e^+e^- \rightarrow \nu_e\bar{\nu}_e$ becomes significant for centre-of-mass energies far above the Z pole and involves as well the γWW vertex.

In general the vertices γWW and ZWW are parametrised in terms of seven triple-gauge-boson couplings (TGCs) each [3], too many to be measured simultaneously. Regarding only CP-conserving couplings and assuming electromagnetic gauge invariance, six TGCs remain, which are g_1^Z, g_5^Z, κ_γ, λ_γ, κ_Z and λ_Z. Within the SM, $g_1^Z = \kappa_\gamma = \kappa_Z = 1$ and $g_5^Z = \lambda_\gamma = \lambda_Z = 0$ at tree level. Except g_5^Z these TGCs also conserve C and P separately.

Assuming custodial SU(2) symmetry leads to the constraints $\Delta\kappa_Z = \Delta g_1^Z - \Delta\kappa_\gamma \tan^2\theta_w$ and $\lambda_Z = \lambda_\gamma$ [4–7], where Δ denotes the deviation of the TGC from its SM value and θ_w is the weak mixing angle. When these constraints are applied, the remaining three TGCs, g_1^Z, κ_γ and λ_γ, correspond to the operators in a linear realization of a gauge-invariant effective Lagrangian that do not affect the gauge-boson propagators at tree level [7]. The TGCs are related to the three α couplings used in our previous publications [8, 9].[1)]

Alternatively, it is interesting to study the TGCs g_1^Z, κ_γ and κ_Z, imposing $\lambda_\gamma = \lambda_Z = 0$. This set corresponds to the operators of lowest dimensionality in the non-linear realization of a gauge-invariant effective Lagrangian, necessary in the absence of a light Higgs boson [7].

In this article we report on measurements of TGCs of the W boson in data samples corresponding to total luminosities of 10.9 pb^{-1}, 10.3 pb^{-1} and 55.5 pb^{-1} collected at centre-of-mass energies of 161 GeV, 172 GeV and 183 GeV, respectively. The results on TGCs are based on analyses of multi-differential cross sections in W-pair, single-W and single-photon production. They include and supersede our previously published results on TGCs [8–10]. Other experiments at LEP and at hadron colliders have also reported results on TGCs [11–14].

2 Event Selection and Reconstruction

The event selections used here are identical to those published earlier on W-pair production [8, 15, 16], single-W production [10], and single-photon production [17]. The same signal and background Monte Carlo and detector simulations are used. The number of selected events and the expected background are reported in Table 1.

[1)] The relations are [7]: $\alpha_{W\Phi} = \Delta g_1^Z \cos^2\theta_w$, $\alpha_{B\Phi} = \Delta\kappa_\gamma - \Delta g_1^Z \cos^2\theta_w$, and $\alpha_W = \lambda_\gamma$.

2.1 W-Pair Events

Each W boson decays into a fermion and an antifermion, for short denoted as qq or $\ell\nu$ in the following. The visible particles in the final state, *i.e.*, electrons, muons, τ jets corresponding to the visible τ decay products, and hadronic jets corresponding to quarks are reconstructed [8, 15, 16]. For $qqqq$ and $qq\ell\nu$ events, energy-momentum conservation and equal mass for the two W bosons are used as constraints in a kinematic fit to determine the kinematics of all four final-state fermions with improved resolution [18].

In the case of $qqqq$ events, a combinatorial ambiguity arises in the assignment of jets to W bosons. The four jets are paired to two W bosons following the criterion of smallest mass difference between the W candidates, excluding the combination with the smallest sum of W masses. On Monte Carlo events, the resulting pairing is found to be correct for 74% of all selected $qqqq$ events at $\sqrt{s} = 183$ GeV [16].

Summing over final-state fermion helicities, fixing the mass of the W boson and neglecting photon radiation, five phase-space angles completely describe the four-fermion final state from W-pair decay for unpolarised initial states. These are the polar scattering angle of the W^- boson, Θ_W, and the polar and azimuthal decay angles in the rest systems of the two decaying W bosons, $\theta_\pm$ and $\phi_\pm$, for the fermion in W^- and the antifermion in W^+ decay. TGCs affect the total production cross section, the distribution of the W-boson polar scattering angle, and the polarisations of the two W bosons, analysed in the distributions of the W decay angles.

For the 161 GeV W-pair data, only the total W-pair cross section is used [8], while at higher centre-of-mass energies also distributions in phase-space angles are analysed. For charged leptons, the sign of their electric charge determines whether they are fermions or antifermions. For hadronic jets, the flavour and charge of the original quark is not measured. Thus, a two-fold ambiguity arises in the decay angles of hadronically decaying W bosons.

In $qqqq$ events the charges of the two pairs of jets are evaluated, based on a jet-charge technique [9], to assign positive and negative charge to the reconstructed W bosons. For events with correctly paired jets, the W charge assignment is found to be correct in 69% of all selected $qqqq$ events at $\sqrt{s} = 183$ GeV. The distribution of the W^- polar scattering angle, Θ_W, shown in Figure 1a, and the total cross section are used for the determination of TGCs.

In $qq\ell\nu$ events the W charge assignment is given by the charge of the lepton. The total cross section and the threefold differential distribution in the W^- polar scattering angle, Θ_W, and the two decay angles of the leptonically decaying W boson, θ_ℓ and ϕ_ℓ, are used for the determination of TGCs. The corresponding three one-dimensional projections are shown in Figures 1b and 2.

In $\ell\nu\ell\nu$ events two unmeasured neutrinos are present. Knowing the momentum and charge of both charged leptons, it is possible to calculate the polar scattering angle of the W^- boson up to a twofold ambiguity arising from the solutions of a quadratic equation. This requires imposing energy-momentum conservation, fixing the masses of the two W bosons to $M_W = 80.41$ GeV [19], and neglecting photon radiation. Both solutions are considered, each weighted by a factor of 0.5. In two cases the true W polar angle is not reconstructed: (1) if one or both of the leptons is a τ, the visible lepton energy entering the calculation is not the energy of the produced τ lepton; (2) if the two solutions are complex, which occurs in 23% of the selected $\ell\nu\ell\nu$ events, their imaginary parts are dropped. However, the distributions still show sensitivity to TGCs. The distribution of the polar scattering angle, Θ_W, shown in Figure 1c, and the total cross section are used for the determination of TGCs.

2.2 Single-W Events

If in the process $e^+e^- \to We\nu$ the final state electron is scattered at low polar angles, it escapes detection along the beam pipe. Only the decay products of a single W boson are observed.

Leptonic single-W events, where the W boson decays into a lepton-neutrino pair, are selected by requiring a single charged lepton, either electron, muon or τ jet, without any other activity in the detector [10]. Only the total cross section is used in the determination of TGCs.

Hadronic single-W events, where the W boson decays into a quark pair, are selected with a neural network approach [10]. After a preselection, several kinematic variables are fed into a neural network trained to separate the hadronic single-W events from the dominating background of $qq\ell\nu$ W-pair events. The total cross section and the distribution of the neural-network output variable are used in the determination of TGCs.

About a third of the hadronic single-W events are also selected by the $qq\ell\nu$ W-pair selections, see Table 2, mainly $qq\tau\nu$ events. In order to avoid double counting, such events are considered in the W-pair sample only. This reduces the sensitivity of the single-W sample to TGCs as compared to the sensitivity obtained in our published single-W TGC analysis [10]. However, in combination with the W-pair signal the overall sensitivity is expected to be better than that achieved when removing the duplicate events from the $qq\ell\nu$ W-pair samples. The resulting distribution of the output of the neural network is shown in Figure 3.

2.3 Single-Photon Events

Single-photon events are selected by requiring one energy deposition above 5 GeV inside a polar angular range from 14° to 166° in the electromagnetic calorimeter with an electromagnetic shower shape and without any other activity in the detector [17]. Because of azimuthal symmetry, there are two relevant observables for single-photon events, the energy and the polar angle of the single photon.

The total cross section and the shape of the twofold differential distribution in these two observables are used in the determination of TGCs. The corresponding two one-dimensional projections are shown in Figure 4. The main sensitivity of single-photon events to TGCs occurs at high photon energies above those corresponding to the radiative return to the Z.

3 Fitting Method

The fitting procedure uses the maximum likelihood method to extract values and errors for one or more of the TGCs denoted as Ψ for short in the following. It is similar to the fitting procedure used in our analysis for the mass and width of the W boson [18].

For each data event, the fit considers the set of values of the reconstructed observables, Ω, as discussed in Sections 2.1, 2.2 and 2.3. The likelihood is the product of the normalised differential cross section, $L(\Omega, \Psi)$, for all data events, calculated as a function of the TGCs Ψ to be fitted. For a given final state i, one has:

$$L_i(\Omega_i, \Psi) = \frac{1}{\sigma_i^{\mathrm{sig}}(\Psi) + \sigma_i^{\mathrm{bg}}(\Psi)} \left[\frac{\mathrm{d}\sigma_i^{\mathrm{sig}}(\Omega_i, \Psi)}{\mathrm{d}\Omega_i} + \frac{\mathrm{d}\sigma_i^{\mathrm{bg}}(\Omega_i, \Psi)}{\mathrm{d}\Omega_i} \right], \tag{1}$$

where σ_i^{sig} and σ_i^{bg} are the accepted signal and background cross sections. For the background which is independent of the TGCs Ψ, the total and differential cross sections are taken from Monte Carlo simulations.

For values $\Psi_{\rm fit}$ varied during the fitting procedure, the Ψ-dependent total and differential signal and background cross sections are determined by a reweighting procedure applied to Monte Carlo events originally generated with TGC values $\Psi_{\rm gen}$. The event weights R_i are calculated as the ratio:

$$R_i(p_n, \Psi_{\rm fit}, \Psi_{\rm gen}) \quad = \quad \frac{|\mathcal{M}_i(p_n, \Psi_{\rm fit})|^2}{|\mathcal{M}_i(p_n, \Psi_{\rm gen})|^2}\,, \qquad (2)$$

where $\mathcal{M}_i$ is the matrix element of the considered final state i evaluated for the generated four-momenta p_n including radiated photons. For W-pair and single-W events the matrix elements as implemented in the EXCALIBUR [20] event generator are used, which include all relevant tree-level Feynman diagrams contributing to a given four-fermion final state. The reweighting procedure is checked by comparisons with GENTLE [21] and GRC4F [22] cross section predictions, especially important in the case of single-W production as GRC4F includes the effects of fermion masses. In the case of single-photon production the matrix element as implemented in KORALZ [23] is used. The reweighting procedure is tested by comparing reweighted distributions to distributions generated with NNGPV [24] at various values of TGCs. In all cases good agreement is observed.

The total accepted cross section for a given set of parameters $\Psi_{\rm fit}$ is then:

$$\sigma_i(\Psi_{\rm fit}) \quad = \quad \frac{\sigma_i^{\rm gen}}{N_i^{\rm gen}} \cdot \sum_j R_i(j, \Psi_{\rm fit}, \Psi_{\rm gen})\,, \qquad (3)$$

where $\sigma_i^{\rm gen}$ denotes the cross section corresponding to the total Monte Carlo sample containing $N_i^{\rm gen}$ events. The sum extends over all accepted Monte Carlo events j. The accepted differential cross section in reconstructed quantities Ω_i is determined by averaging Monte Carlo events inside a box in Ω_i around each data event [25]:

$$\frac{d\sigma_i(\Omega_i, \Psi_{\rm fit})}{d\Omega_i} \quad = \quad \frac{\sigma_i^{\rm gen}}{N_i^{\rm gen}} \cdot \frac{1}{\Delta_i^\Omega} \sum_{j \epsilon \Delta_i^\Omega} R_i(j, \Psi_{\rm fit}, \Psi_{\rm gen})\,, \qquad (4)$$

where Δ_i^Ω is the volume of the box and the sum extends over all accepted Monte Carlo events j inside the box. This takes Ω_i-dependent detector effects and Ψ-dependent efficiencies and purities properly into account. The boxes are constructed in such a way that the Monte Carlo events in the box are the 200 events closest to the data point. The box size in each of the observables is proportional to the experimental resolution in those variables.

Extended maximum likelihood fits are performed, including the overall normalisations according to the measured total cross sections. The likelihood is multiplied by the Poissonian probability to obtain the numbers of events observed in the data, given the luminosity and the expectations for the accepted signal and background cross sections, $\sigma_i^{\rm sig}(\Psi_{\rm fit})$ and $\sigma_i^{\rm bg}(\Psi_{\rm fit})$.

The fitting method described above determines the TGCs without any bias as long as the Monte Carlo describes photon radiation and detector effects such as resolution and acceptance functions correctly. By fitting large Monte Carlo samples, typically a hundred times the data, the fitting procedure is tested to high accuracy. The fits reproduce well the values of the TGCs of the large Monte Carlo samples being fitted, varied in a range corresponding to three times the error expected for the size of the data samples analysed. Also, the fit results do not depend on the values of the TGCs $\Psi_{\rm gen}$ of the Monte Carlo sample subjected to the reweighting procedure.

The reliability of the statistical errors as given by the fit is tested by fitting for each final state several hundred small Monte Carlo samples, each the size of the data samples. The width of the distribution of the fitted central values agrees well with the mean of the distribution of the fitted errors.

4 Triple-Gauge-Boson Couplings of the W Boson

In W-pair, single-W and single-photon production, the triple-gauge-boson vertices are tested at different momentum-transfer scales Q^2. For each TGC investigated, the results derived at $Q^2 = s$ from W-pair production, at $Q^2 = M_\mathrm{W}^2$ from single-W production, and at $Q^2 = 0$ from single-photon production are in good agreement with each other, as shown in Table 3 and Figure 5. No Q^2 dependence is observed. Combined results, obtained by adding the individual log-likelihood functions as shown in Figure 5, are reported in Tables 3 and 4. Compared to the current level of statistical accuracy, the Q^2 dependence of the TGCs expected in the SM is negligible [3] and is thus ignored in the combination. As a cross check, the method of optimal observables [26, 27] is used in the case of $qq\ell\nu$ W-pair events at $\sqrt{s} = 183$ GeV. Compatible results are obtained.

The statistical errors on TGCs observed in W-pair production are larger than the expected statistical errors which are also reported in Table 3. The large total cross section measured in the $qqqq$ W-pair process at $\sqrt{s} = 183$ GeV [16] and the quadratic dependence of the theoretical W-pair cross section on the TGCs cause the negative log-likelihood functions for this final state to exhibit a two-minima structure. Thus the sum of all log-likelihood functions has a smaller curvature than expected with SM cross sections. Expected errors calculated based on the observed cross sections agree well with the observed errors.

Multi-parameter fits of TGCs are also performed, which allow for a more model-independent general interpretation of the data. Fits to two of the three C- and P-conserving TGCs g_1^Z, κ_γ, and λ_γ, keeping the third fixed at its SM value, as well as a fit to all three of these TGCs are performed. In each case the constraints $g_5^\mathrm{Z} = 0$, $\Delta\kappa_\mathrm{Z} = \Delta g_1^\mathrm{Z} - \Delta\kappa_\gamma \tan^2\theta_w$ and $\lambda_\mathrm{Z} = \lambda_\gamma$ are imposed. A three-parameter fit to the TGCs g_1^Z, κ_γ and κ_Z is also performed, now imposing the constraints $g_5^\mathrm{Z} = \lambda_\gamma = \lambda_\mathrm{Z} = 0$ instead. For the four-parameter fit to $(\kappa_\gamma, \lambda_\gamma, \kappa_\mathrm{Z}, \lambda_\mathrm{Z})$, the constraints between the γWW and the ZWW couplings are removed while the constraints $g_1^\mathrm{Z} = 1$ and $g_5^\mathrm{Z} = 0$ are imposed. The numerical results of all multi-parameter fits to TGCs including the correlation matrices are reported in Table 4.

As an example, the contour curves of 68% and 95% probability derived from fits to two of the three C- and P-conserving TGCs g_1^Z, κ_γ, and λ_γ, keeping the third fixed at its SM value, are shown in Figure 6. The contour curves correspond to a change in log-likelihood with respect to its minimum of 1.15 and 3.0, respectively.

4.1 Systematic Errors

The sources of systematic errors considered include those studied for the W-boson mass and width analysis [18]: LEP energy, initial- and final-state radiation, jet and lepton measurement, fragmentation and decay, background normalisation and shape, Monte Carlo statistics, fitting method, and in the case of the $qqqq$ final state, colour reconnection and Bose-Einstein effects. The methods used to evaluate the effects on TGCs are identical. The changes in both the central value and the statistical error due to systematic effects are taken into account.

The systematic errors on TGCs for the different models and processes are summarised in Tables 5 and 6. In most cases the total systematic error is dominated by the uncertainty in the experimental selection efficiencies and the theoretical error of 2% on the total cross section predictions. Additional systematic effects arise due to uncertainties in the description of the charge confusion affecting the W charge assignment. Systematic errors due to uncertainties in the mass and total width of the W boson are small.

4.2 Results and Discussion

For the CP conserving but C- and P-violating coupling g_5^Z, the following result is obtained when all other TGCs are fixed to their SM values:

$$g_5^Z = -0.44^{+0.23}_{-0.22} \pm 0.12\,. \tag{5}$$

The first error is statistical and the second systematic. The result is in agreement with the SM expectation of $g_5^Z = 0$. Imposing the constraints $g_5^Z = 0$, $\Delta\kappa_Z = \Delta g_1^Z - \Delta\kappa_\gamma \tan^2\theta_w$ and $\lambda_Z = \lambda_\gamma$, three C- and P-conserving TGCs remain. The results of fits to the individual couplings, keeping the other two at their SM values, are:

$$g_1^Z = +1.11^{+0.19}_{-0.18} \pm 0.10 \tag{6}$$
$$\kappa_\gamma = +1.11^{+0.25}_{-0.25} \pm 0.17 \tag{7}$$
$$\lambda_\gamma = +0.10^{+0.22}_{-0.20} \pm 0.10\,. \tag{8}$$

The log-likelihood functions for all four one-parameter fits are shown in Figure 5. The contribution from W-pair production dominates in the case of g_5^Z, g_1^Z and λ_γ, while the single-W contribution is important for the constraint on κ_γ. The hadronic single-W samples also contribute to the constraints on the ZWW couplings through the remaining couplings-dependent $qq\ell\nu$ W-pair background. The single-photon samples constrain the γWW couplings only.

All single- and multi-parameter TGC results show good agreement with the SM expectation and imply the existence of the self coupling among the electroweak gauge bosons. The resulting constraints on non-SM contributions to TGCs are significantly improved with respect to our previous analyses [8–10].

The measurements exclude a theory by Klein [28], predicting a value of $\kappa_\gamma = -2$, by more than ten standard deviations. If the W boson were an extended object, *e.g.*, an ellipsoid of rotation with longitudinal radius a and transverse radius b, its typical size and shape would be related to the TGCs by $R_W \equiv (a+b)/2 = (\kappa_\gamma + \lambda_\gamma - 1)/M_W$ [29] and $\Delta_W \equiv (a^2 - b^2)/2 = (5/4)(\kappa_\gamma - \lambda_\gamma - 1)/M_W^2$ [30–32]. The measurements show no evidence for the W boson to be an extended object:

$$R_W = (0.3 \pm 1.0) \cdot 10^{-18}\ \mathrm{m} \tag{9}$$
$$\Delta_W = (0.3 \pm 3.1) \cdot 10^{-36}\ \mathrm{m}^2\,, \tag{10}$$

with a correlation coefficient of -0.26. These results establish the pointlike nature of the W boson down to a scale of 10^{-18} m.

5 Acknowledgements

We wish to congratulate the CERN accelerator divisions for the successful upgrade of the LEP machine and to express our gratitude for its good performance. We acknowledge with appreciation the effort of the engineers, technicians and support staff who have participated in the construction and maintenance of this experiment.

References

[1] F. Boudjema *et al.*, in *Physics at LEP 2*, Report CERN 96-01 (1996), eds G. Altarelli, T. Sjöstrand, F. Zwirner, Vol. 1, p. 207.

[2] S. L. Glashow, Nucl. Phys. **22** (1961) 579;
S. Weinberg, Phys. Rev. Lett. **19** (1967) 1264;
A. Salam, in *Elementary Particle Theory*, ed. N. Svartholm, Stockholm, Almquist and Wiksell (1968), 367.

[3] K. Hagiwara, R.D. Peccei, D. Zeppenfeld and K. Hikasa, Nucl. Phys. **B 282** (1987) 253.

[4] K. Gaemers and G. Gounaris, Z. Phys. **C 1** (1979) 259.

[5] M. Bilenky, J.L. Kneur, F.M. Renard and D. Schildknecht, Nucl. Phys. **B 409** (1993) 22; Nucl. Phys. **B 419** (1994) 240.

[6] I. Kuss and D. Schildknecht, Phys. Lett. **B 383** (1996) 470.

[7] G. Gounaris *et al.*, in *Physics at LEP 2*, Report CERN 96-01 (1996), eds G. Altarelli, T. Sjöstrand, F. Zwirner, Vol. 1, p. 525.

[8] The L3 Collaboration, M. Acciarri *et al.*, Phys. Lett. **B 398** (1997) 223.

[9] The L3 Collaboration, M. Acciarri *et al.*, Phys. Lett. **B 413** (1997) 176.

[10] The L3 Collaboration, M. Acciarri *et al.*, Phys. Lett. **B 403** (1997) 168; Phys. Lett. **B 436** (1998) 417.

[11] The ALEPH Collaboration, R. Barate *et al.*, Phys. Lett. **B 422** (1998) 369; Phys. Lett. **B 445** (1998) 239; CERN-EP/99-086 (1999).

[12] The DELPHI Collaboration, P. Abreu *et al.*, Phys. Lett. **B 397** (1997) 158; Phys. Lett. **B 423** (1998) 194; Phys. Lett. **B 459** (1999) 382.

[13] The OPAL Collaboration, K. Ackerstaff *et al.*, Phys. Lett. **B 397** (1997) 147; Euro. Phys. Jour. **C 2** (1998) 597; G. Abbiendi *et al.*, Eur.Phys.Jour. **C 8** (1999) 191.

[14] The UA2 Collaboration, J. Alitti *et al.*, Phys. Lett. **B 277** (1992) 194.
The CDF Collaboration, F. Abe *et al.*, Phys. Rev. Lett. **74** (1995) 1936; Phys. Rev. Lett. **75** (1995) 1017; Phys. Rev. Lett. **78** (1997) 4536.
The DØ Collaboration, S. Abachi *et al.*, Phys. Rev. Lett. **75** (1995) 1023; Phys. Rev. Lett. **75** (1995) 1028; Phys. Rev. Lett. **75** (1995) 1034; Phys. Rev. Lett. **77** (1996) 3303; Phys. Rev. Lett. **78** (1997) 3634; Phys. Rev. Lett. **78** (1997) 3640; Phys. Rev. **D 56** (1997) 6742; B. Abbott *et al.*, Phys. Rev. Lett. **79** (1997) 1441; Phys. Rev. **D 58** (1998) 031102; Phys. Rev. **D 58** (1998) 051101; hep-ex/9905005 submitted to Phys. Rev. D.

[15] The L3 Collaboration, M. Acciarri *et al.*, Phys. Lett. **B 407** (1997) 419.

[16] The L3 Collaboration, M. Acciarri *et al.*, Phys. Lett. **B 436** (1998) 437.

[17] The L3 Collaboration, M. Acciarri *et al.*, Phys. Lett. **B 415** (1997) 299; Phys. Lett. **B 444** (1998) 503.

[18] The L3 Collaboration, M. Acciarri *et al.*, Phys. Lett. **B 454** (1999) 386.

[19] C. Caso *et al.*, *The 1998 Review of Particle Physics*, Euro. Phys. Jour. **C 3** (1998) 1.

[20] F.A. Berends, R. Kleiss and R. Pittau, Nucl. Phys. **B 424** (1994) 308; Nucl. Phys. **B 426** (1994) 344; Nucl. Phys. (Proc. Suppl.) **B 37** (1994) 163;
R. Kleiss and R. Pittau, Comp. Phys. Comm. **83** (1994) 141;
R. Pittau, Phys. Lett. **B 335** (1994) 490.

[21] GENTLE version 2.0 is used. D. Bardin *et al.*, Comp. Phys. Comm. **104** (1997) 161.

[22] J. Fujimoto et. al., Comp. Phys. Comm. **100** (1997) 128.

[23] KORALZ version 4.03 is used.
S. Jadach, B. F. L. Ward and Z. Wąs, Comp. Phys. Comm. **79** (1994) 503.

[24] G. Montagna, M. Moretti, O. Nicrosini and F. Piccinini, Nucl. Phys. **B 541** (1999) 31.

[25] D.M. Schmidt, R.J. Morrison and M.S. Witherell, Nucl. Instr. and Meth. **A 328** (1993) 547.

[26] M. Davier, L. Duflot, F. Le Diberder and A. Rouge, Phys. Lett. **B306** (1993) 411–417.

[27] M. Diehl and O. Nachtmann, Z. Phys. **C62** (1994) 397–412.

[28] O. Klein, Surveys High Energ. Phys. **5** (1986) 269, Reprint of the article submitted to the conference “New Theories in Physics”, Warsaw, Poland, May 30 – June 3, 1938.

[29] S. J. Brodsky and S. D. Drell, Phys. Rev. **D22** (1980) 2236.

[30] H. Frauenfelder and E.M. Henley, Subatomic physics, (Englewood Cliffs, New Jersey, 1974).

[31] P. Brix, Z. Naturforschung **A41** (1985) 3.

[32] A. J. Buchmann, Phys. Blätter **1/99** (1999) 47.

The L3 Collaboration:

M.Acciarri,[26] P.Achard,[19] O.Adriani,[16] M.Aguilar-Benitez,[25] J.Alcaraz,[25] G.Alemanni,[22] J.Allaby,[17] A.Aloisio,[28] M.G.Alviggi,[28] G.Ambrosi,[19] H.Anderhub,[47] V.P.Andreev,[6,36] T.Angelescu,[12] F.Anselmo,[9] A.Arefiev,[27] T.Azemoon,[3] T.Aziz,[10] P.Bagnaia,[35] L.Baksay,[42] A.Balandras,[4] R.C.Ball,[3] S.Banerjee,[10] Sw.Banerjee,[10] A.Barczyk,[47,45] R.Barillère,[17] L.Barone,[35] P.Bartalini,[22] M.Basile,[9] R.Battiston,[32] A.Bay,[22] F.Becattini,[16] U.Becker,[14] F.Behner,[47] L.Bellucci,[16] J.Berdugo,[25] P.Berges,[14] B.Bertucci,[32] B.L.Betev,[47] S.Bhattacharya,[10] M.Biasini,[32] A.Biland,[47] J.J.Blaising,[4] S.C.Blyth,[33] G.J.Bobbink,[2] A.Böhm,[1] L.Boldizsar,[13] B.Borgia,[35] D.Bourilkov,[47] M.Bourquin,[19] S.Braccini,[19] J.G.Branson,[38] V.Brigljevic,[47] F.Brochu,[4] A.Buffini,[16] A.Buijs,[43] J.D.Burger,[14] W.J.Burger,[32] J.Busenitz,[42] A.Button,[3] X.D.Cai,[14] M.Campanelli,[47] M.Capell,[14] G.Cara Romeo,[9] G.Carlino,[28] A.M.Cartacci,[16] J.Casaus,[25] G.Castellini,[16] F.Cavallari,[35] N.Cavallo,[28] C.Cecchi,[19] M.Cerrada,[25] F.Cesaroni,[23] M.Chamizo,[19] Y.H.Chang,[49] U.K.Chaturvedi,[18] M.Chemarin,[24] A.Chen,[49] G.Chen,[7] G.M.Chen,[7] H.F.Chen,[20] H.S.Chen,[7] X.Chereau,[4] G.Chiefari,[28] L.Cifarelli,[37] F.Cindolo,[9] C.Civinini,[16] I.Clare,[14] R.Clare,[14] G.Coignet,[4] A.P.Colijn,[2] N.Colino,[25] S.Costantini,[8] F.Cotorobai,[12] B.Cozzoni,[9] B.de la Cruz,[25] A.Csilling,[13] S.Cucciarelli,[32] T.S.Dai,[14] J.A.van Dalen,[30] R.D'Alessandro,[16] R.de Asmundis,[28] P.Déglon,[19] A.Degré,[4] K.Deiters,[45] D.della Volpe,[28] P.Denes,[34] F.DeNotaristefani,[35] A.De Salvo,[47] M.Diemoz,[35] D.van Dierendonck,[2] F.Di Lodovico,[47] C.Dionisi,[35] M.Dittmar,[47] A.Dominguez,[38] A.Doria,[28] M.T.Dova,[18,♯] D.Duchesneau,[4] S.Duensing,[8] D.Dufournaud,[4] P.Duinker,[2] I.Duran,[39] H.El Mamouni,[24] A.Engler,[33] F.J.Eppling,[14] F.C.Erné,[2] P.Extermann,[19] M.Fabre,[45] R.Faccini,[35] M.A.Falagan,[25] S.Falciano,[35,17] A.Favara,[17] J.Fay,[24] O.Fedin,[36] M.Felcini,[47] T.Ferguson,[33] F.Ferroni,[35] H.Fesefeldt,[1] E.Fiandrini,[32] J.H.Field,[19] F.Filthaut,[17] P.H.Fisher,[14] I.Fisk,[38] G.Forconi,[14] L.Fredj,[19] K.Freudenreich,[47] C.Furetta,[26] Yu.Galaktionov,[27,14] S.N.Ganguli,[10] P.Garcia-Abia,[5] M.Gataullin,[31] S.S.Gau,[11] S.Gentile,[35,17] N.Gheordanescu,[12] S.Giagu,[35] Z.F.Gong,[20] G.Grenier,[24] O.Grimm,[47] M.W.Gruenewald,[8] M.Guida,[37] R.van Gulik,[2] V.K.Gupta,[34] A.Gurtu,[10] L.J.Gutay,[44] D.Haas,[5] A.Hasan,[29] D.Hatzifotiadou,[9] T.Hebbeker,[8] A.Hervé,[17] P.Hidas,[13] J.Hirschfelder,[33] H.Hofer,[47] G. Holzner,[47] H.Hoorani,[33] S.R.Hou,[49] I.Iashvili,[46] B.N.Jin,[7] L.W.Jones,[3] P.de Jong,[2] I.Josa-Mutuberría,[25] R.A.Khan,[18] D.Kamrad,[46] M.Kaur,[18,◇] M.N.Kienzle-Focacci,[19] D.Kim,[35] D.H.Kim,[41] J.K.Kim,[41] S.C.Kim,[41] J.Kirkby,[17] D.Kiss,[13] W.Kittel,[30] A.Klimentov,[14,27] A.C.König,[30] A.Kopp,[46] I.Korolko,[27] V.Koutsenko,[14,27] M.Kräber,[47] R.W.Kraemer,[33] W.Krenz,[1] A.Kunin,[14,27] P.Ladron de Guevara,[25] I.Laktineh,[24] G.Landi,[16] K.Lassila-Perini,[47] P.Laurikainen,[21] A.Lavorato,[37] M.Lebeau,[17] A.Lebedev,[14] P.Lebrun,[24] P.Lecomte,[47] P.Lecoq,[17] P.Le Coultre,[47] H.J.Lee,[8] J.M.Le Goff,[17] R.Leiste,[46] E.Leonardi,[35] P.Levtchenko,[36] C.Li,[20] C.H.Lin,[49] W.T.Lin,[49] F.L.Linde,[2] L.Lista,[28] Z.A.Liu,[7] W.Lohmann,[46] E.Longo,[35] Y.S.Lu,[7] K.Lübelsmeyer,[1] C.Luci,[17,35] D.Luckey,[14] L.Lugnier,[24] L.Luminari,[35] W.Lustermann,[47] W.G.Ma,[20] M.Maity,[10] L.Malgeri,[17] A.Malinin,[27,17] C.Maña,[25] D.Mangeol,[30] P.Marchesini,[47] G.Marian,[15] J.P.Martin,[24] F.Marzano,[35] G.G.G.Massaro,[2] K.Mazumdar,[10] R.R.McNeil,[6] S.Mele,[17] L.Merola,[28] M.Meschini,[16] W.J.Metzger,[30] M.von der Mey,[1] A.Mihul,[12] H.Milcent,[17] G.Mirabelli,[35] J.Mnich,[17] G.B.Mohanty,[10] P.Molnar,[8] B.Monteleoni,[16,†] T.Moulik,[10] G.S.Muanza,[24] F.Muheim,[19] A.J.M.Muijs,[2] M.Musy,[35] M.Napolitano,[28] F.Nessi-Tedaldi,[47] H.Newman,[31] T.Niessen,[1] A.Nisati,[35] H.Nowak,[46] Y.D.Oh,[41] G.Organtini,[35] R.Ostonen,[21] C.Palomares,[25] D.Pandoulas,[1] S.Paoletti,[35,17] P.Paolucci,[28] R.Paramatti,[35] H.K.Park,[33] I.H.Park,[41] G.Pascale,[35] G.Passaleva,[17] S.Patricelli,[28] T.Paul,[11] M.Pauluzzi,[32] C.Paus,[17] F.Pauss,[47] D.Peach,[17] M.Pedace,[35] S.Pensotti,[26] D.Perret-Gallix,[4] B.Petersen,[30] D.Piccolo,[28] F.Pierella,[9] M.Pieri,[16] P.A.Piroué,[34] E.Pistolesi,[26] V.Plyaskin,[27] M.Pohl,[47] V.Pojidaev,[27,16] H.Postema,[14] J.Pothier,[17] N.Produit,[19] D.O.Prokofiev,[44] D.Prokofiev,[36] J.Quartieri,[37] G.Rahal-Callot,[47,17] M.A.Rahaman,[10] P.Raics,[15] N.Raja,[10] R.Ramelli,[47] P.G.Rancoita,[26] G.Raven,[38] P.Razis,[29]D.Ren,[47] M.Rescigno,[35] S.Reucroft,[11] T.van Rhee,[43] S.Riemann,[46] K.Riles,[3] A.Robohm,[47] J.Rodin,[42] B.P.Roe,[3] L.Romero,[25] A.Rosca,[8] S.Rosier-Lees,[4] J.A.Rubio,[17] D.Ruschmeier,[8] H.Rykaczewski,[47] S.Saremi,[6] S.Sarkar,[35] J.Salicio,[17] E.Sanchez,[17] M.P.Sanders,[30] M.E.Sarakinos,[21] C.Schäfer,[1] V.Schegelsky,[36] S.Schmidt-Kaerst,[1] D.Schmitz,[1] H.Schopper,[48] D.J.Schotanus,[30] G.Schwering,[1] C.Sciacca,[28] D.Sciarrino,[19] A.Seganti,[9] L.Servoli,[32] S.Shevchenko,[31] N.Shivarov,[40] V.Shoutko,[27] E.Shumilov,[27] A.Shvorob,[31] T.Siedenburg,[1] D.Son,[41] B.Smith,[33] P.Spillantini,[16] M.Steuer,[14] D.P.Stickland,[34] A.Stone,[6] H.Stone,[34,†] B.Stoyanov,[40] A.Straessner,[1] K.Sudhakar,[10] G.Sultanov,[18] L.Z.Sun,[20] H.Suter,[47] J.D.Swain,[18] Z.Szillasi,[42,¶] T.Sztaricskai,[42,¶] X.W.Tang,[7] L.Tauscher,[5] L.Taylor,[11] C.Timmermans,[30] Samuel C.C.Ting,[14] S.M.Ting,[14] S.C.Tonwar,[10] J.Tóth,[13] C.Tully,[34] K.L.Tung,[7]Y.Uchida,[14] J.Ulbricht,[47] E.Valente,[35] G.Vesztergombi,[13] I.Vetlitsky,[27] D.Vicinanza,[37] G.Viertel,[47] S.Villa,[11] M.Vivargent,[4] S.Vlachos,[5] I.Vodopianov,[36] H.Vogel,[33] H.Vogt,[46] I.Vorobiev,[27] A.A.Vorobyov,[36] A.Vorvolakos,[29] M.Wadhwa,[5] W.Wallraff,[1] M.Wang,[14] X.L.Wang,[20] Z.M.Wang,[20] A.Weber,[1] M.Weber,[1] P.Wienemann,[1] H.Wilkens,[30] S.X.Wu,[14] S.Wynhoff,[1] L.Xia,[31] Z.Z.Xu,[20] B.Z.Yang,[20] C.G.Yang,[7] H.J.Yang,[7] M.Yang,[7] J.B.Ye,[20] S.C.Yeh,[50] An.Zalite,[36] Yu.Zalite,[36] Z.P.Zhang,[20] G.Y.Zhu,[7] R.Y.Zhu,[31] A.Zichichi,[9,17,18] F.Ziegler,[46] G.Zilizi,[42,¶] M.Zöller.[1]

1 I. Physikalisches Institut, RWTH, D-52056 Aachen, FRG[§]
III. Physikalisches Institut, RWTH, D-52056 Aachen, FRG[§]
2 National Institute for High Energy Physics, NIKHEF, and University of Amsterdam, NL-1009 DB Amsterdam, The Netherlands
3 University of Michigan, Ann Arbor, MI 48109, USA
4 Laboratoire d'Annecy-le-Vieux de Physique des Particules, LAPP,IN2P3-CNRS, BP 110, F-74941 Annecy-le-Vieux CEDEX, France
5 Institute of Physics, University of Basel, CH-4056 Basel, Switzerland
6 Louisiana State University, Baton Rouge, LA 70803, USA
7 Institute of High Energy Physics, IHEP, 100039 Beijing, China[△]
8 Humboldt University, D-10099 Berlin, FRG[§]
9 University of Bologna and INFN-Sezione di Bologna, I-40126 Bologna, Italy
10 Tata Institute of Fundamental Research, Bombay 400 005, India
11 Northeastern University, Boston, MA 02115, USA
12 Institute of Atomic Physics and University of Bucharest, R-76900 Bucharest, Romania
13 Central Research Institute for Physics of the Hungarian Academy of Sciences, H-1525 Budapest 114, Hungary[‡]
14 Massachusetts Institute of Technology, Cambridge, MA 02139, USA
15 Lajos Kossuth University-ATOMKI, H-4010 Debrecen, Hungary[¶]
16 INFN Sezione di Firenze and University of Florence, I-50125 Florence, Italy
17 European Laboratory for Particle Physics, CERN, CH-1211 Geneva 23, Switzerland
18 World Laboratory, FBLJA Project, CH-1211 Geneva 23, Switzerland
19 University of Geneva, CH-1211 Geneva 4, Switzerland
20 Chinese University of Science and Technology, USTC, Hefei, Anhui 230 029, China[△]
21 SEFT, Research Institute for High Energy Physics, P.O. Box 9, SF-00014 Helsinki, Finland
22 University of Lausanne, CH-1015 Lausanne, Switzerland
23 INFN-Sezione di Lecce and Universitá Degli Studi di Lecce, I-73100 Lecce, Italy
24 Institut de Physique Nucléaire de Lyon, IN2P3-CNRS,Université Claude Bernard, F-69622 Villeurbanne, France
25 Centro de Investigaciones Energéticas, Medioambientales y Tecnologícas, CIEMAT, E-28040 Madrid, Spain♭
26 INFN-Sezione di Milano, I-20133 Milan, Italy
27 Institute of Theoretical and Experimental Physics, ITEP, Moscow, Russia
28 INFN-Sezione di Napoli and University of Naples, I-80125 Naples, Italy
29 Department of Natural Sciences, University of Cyprus, Nicosia, Cyprus
30 University of Nijmegen and NIKHEF, NL-6525 ED Nijmegen, The Netherlands
31 California Institute of Technology, Pasadena, CA 91125, USA
32 INFN-Sezione di Perugia and Universitá Degli Studi di Perugia, I-06100 Perugia, Italy
33 Carnegie Mellon University, Pittsburgh, PA 15213, USA
34 Princeton University, Princeton, NJ 08544, USA
35 INFN-Sezione di Roma and University of Rome, "La Sapienza", I-00185 Rome, Italy
36 Nuclear Physics Institute, St. Petersburg, Russia
37 University and INFN, Salerno, I-84100 Salerno, Italy
38 University of California, San Diego, CA 92093, USA
39 Dept. de Fisica de Particulas Elementales, Univ. de Santiago, E-15706 Santiago de Compostela, Spain
40 Bulgarian Academy of Sciences, Central Lab. of Mechatronics and Instrumentation, BU-1113 Sofia, Bulgaria
41 Center for High Energy Physics, Adv. Inst. of Sciences and Technology, 305-701 Taejon, Republic of Korea
42 University of Alabama, Tuscaloosa, AL 35486, USA
43 Utrecht University and NIKHEF, NL-3584 CB Utrecht, The Netherlands
44 Purdue University, West Lafayette, IN 47907, USA
45 Paul Scherrer Institut, PSI, CH-5232 Villigen, Switzerland
46 DESY, D-15738 Zeuthen, FRG
47 Eidgenössische Technische Hochschule, ETH Zürich, CH-8093 Zürich, Switzerland
48 University of Hamburg, D-22761 Hamburg, FRG
49 National Central University, Chung-Li, Taiwan, China
50 Department of Physics, National Tsing Hua University, Taiwan, China
§ Supported by the German Bundesministerium für Bildung, Wissenschaft, Forschung und Technologie
‡ Supported by the Hungarian OTKA fund under contract numbers T019181, F023259 and T024011.
¶ Also supported by the Hungarian OTKA fund under contract numbers T22238 and T026178.
♭ Supported also by the Comisión Interministerial de Ciencia y Tecnología.
♯ Also supported by CONICET and Universidad Nacional de La Plata, CC 67, 1900 La Plata, Argentina.
◇ Also supported by Panjab University, Chandigarh-160014, India.
△ Supported by the National Natural Science Foundation of China.
† Deceased.

$\sqrt{s}$	183 GeV		172 GeV		161 GeV	
Process	$N_{\rm data}$	$N_{\rm bg}$	$N_{\rm data}$	$N_{\rm bg}$	$N_{\rm data}$	$N_{\rm bg}$
WW $\rightarrow \ell\nu\ell\nu$	54	9.7	19	0.6	2	0.4
WW $\rightarrow qqe\nu$	112	6.7	9	0.4	4	0.2
WW $\rightarrow qq\mu\nu$	108	5.7	12	2.1	4	0.2
WW $\rightarrow qq\tau\nu$	77	10.6	9	0.3	3	1.6
WW $\rightarrow qqqq$	473	81.2	61	12.6	11	5.1
Weν, W $\rightarrow qq$	86	72.6	15	10.1	7	5.5
Weν, W $\rightarrow \ell\nu$	10	3.1	1	0.4	1	0.4
$\nu\bar{\nu}\gamma$	198	2.1	52	0.3	59	0.6

Table 1: Number of selected data events, $N_{\rm data}$, and expected background events, $N_{\rm bg}$, in W-pair, single-W and single-photon production.

$\sqrt{s}$ [GeV]	Initial Sample	Overlap with W-Pairs $qqe\nu$	$qq\mu\nu$	$qq\tau\nu$	Final Sample
183	86	2	9	27	48
172	15	1	—	3	11
161	7	—	—	—	7

Table 2: Number of events selected by the hadronic single-W selection and the overlap with the $qq\ell\nu$ W-pair selections. Duplicate events are removed from the hadronic single-W samples.

Process	Q^2	$g_1^{\rm Z}$	κ_γ	λ_γ	$g_5^{\rm Z}$
$\rm e^+e^- \rightarrow WW$	s	$+1.13^{+0.18}_{-0.18}$	$+1.00^{+0.93}_{-0.39}$	$+0.10^{+0.22}_{-0.20}$	$-0.44^{+0.23}_{-0.22}$
		($\pm$0.13)	($\pm$0.27)	($\pm$0.14)	($\pm$0.17)
$\rm e^+e^- \rightarrow We\nu$	$M_{\rm W}^2$	$+0.57^{+0.93}_{-0.40}$	$+1.12^{+0.27}_{-0.31}$	$-0.52^{+1.16}_{-0.36}$	$-0.55^{+2.24}_{-0.86}$
		($\pm$0.65)	($\pm$0.34)	($\pm$0.54)	($\pm$1.49)
$\rm e^+e^- \rightarrow \nu\bar{\nu}\gamma$	0	—	$+1.26^{+0.96}_{-0.96}$	$+0.41^{+1.26}_{-1.25}$	—
		—	($\pm$1.19)	($\pm$1.49)	—
Combined		$+1.11^{+0.19}_{-0.18}$	$+1.11^{+0.25}_{-0.25}$	$+0.10^{+0.22}_{-0.20}$	$-0.44^{+0.23}_{-0.22}$
		($\pm$0.13)	($\pm$0.21)	($\pm$0.13)	($\pm$0.17)

Table 3: Results of one-parameter fits to the TGCs $g_1^{\rm Z}$, κ_γ, λ_γ, $g_5^{\rm Z}$, derived from W-pair, single-W and single-photon events, and their combination. For each TGC, the other three are set to their SM values and the constraints $\Delta\kappa_{\rm Z} = \Delta g_1^{\rm Z} - \Delta\kappa_\gamma \tan^2\theta_w$ and $\lambda_{\rm Z} = \lambda_\gamma$ are imposed. The errors are statistical. Expected statistical errors are given in parenthesis.

Parameter	g_1^{Z}	κ_γ	λ_γ	κ_{Z}	λ_{Z}
Two-Parameter Fits					
(g_1^{Z},κ_γ)	$+1.11^{+0.18}_{-0.20}$	$+1.07^{+0.29}_{-0.27}$	—	—	—
Corr(g_1^{Z})	1.00	−0.24	—	—	—
(g_1^{Z},λ_γ)	$+1.18^{+0.23}_{-0.43}$	—	$-0.08^{+0.48}_{-0.24}$	—	—
Corr(g_1^{Z})	1.00	—	−0.78	—	—
(κ_γ,λ_γ)	—	$+1.02^{+0.30}_{-0.30}$	$+0.09^{+0.23}_{-0.21}$	—	—
Corr(κ_γ)	—	1.00	−0.35	—	—
Three-Parameter Fits					
(g_1^{Z},κ_γ,λ_γ)	$+0.97^{+0.35}_{-0.30}$	$+1.07^{+0.26}_{-0.27}$	$+0.13^{+0.28}_{-0.39}$	—	—
Corr(g_1^{Z})	1.00	−0.21	−0.80	—	—
Corr(κ_γ)	−0.21	1.00	0.04	—	—
Corr(λ_γ)	−0.80	0.04	1.00	—	—
(g_1^{Z},κ_γ,κ_{Z})	$+1.80^{+0.45}_{-1.23}$	$+1.07^{+0.23}_{-0.24}$	—	$+0.41^{+1.16}_{-0.53}$	—
Corr(g_1^{Z})	1.00	0.07	—	−0.57	—
Corr(κ_γ)	0.07	1.00	—	−0.29	—
Corr(κ_{Z})	−0.57	−0.29	—	1.00	—
Four-Parameter Fit					
(κ_γ,λ_γ,κ_{Z},λ_{Z})	—	$+1.20^{+0.37}_{-0.26}$	$+0.42^{+0.34}_{-0.57}$	$+1.23^{+0.40}_{-0.42}$	$-0.46^{+0.26}_{-0.34}$
Corr(κ_γ)	—	1.00	−0.35	−0.29	−0.30
Corr(λ_γ)	—	−0.35	1.00	−0.10	−0.05
Corr(κ_{Z})	—	−0.29	−0.10	1.00	−0.26
Corr(λ_{Z})	—	−0.30	−0.05	−0.26	1.00

Table 4: Results on the C- and P-conserving TGCs derived from the two- and three-parameter fits to $(g_1^{\mathrm{Z}},\kappa_\gamma)$, $(g_1^{\mathrm{Z}},\lambda_\gamma)$, $(\kappa_\gamma,\lambda_\gamma)$, and $(g_1^{\mathrm{Z}},\kappa_\gamma,\lambda_\gamma)$, imposing the constraints $g_5^{\mathrm{Z}} = 0$, $\Delta\kappa_{\mathrm{Z}} = \Delta g_1^{\mathrm{Z}} - \Delta\kappa_\gamma \tan^2\theta_w$ and $\lambda_{\mathrm{Z}} = \lambda_\gamma$; from the three-parameter fit to $(g_1^{\mathrm{Z}},\kappa_\gamma,\kappa_{\mathrm{Z}})$ imposing the constraints $g_5^{\mathrm{Z}} = \lambda_\gamma = \lambda_{\mathrm{Z}} = 0$; and from the four-parameter fit to $(\kappa_\gamma,\lambda_\gamma,\kappa_{\mathrm{Z}},\lambda_{\mathrm{Z}})$ imposing the constraints $g_5^{\mathrm{Z}} = 0$ and $g_1^{\mathrm{Z}} = 1$. The matrices of correlation coefficients are also given. The errors are statistical, combining all processes.

Process	$g_1^{\rm Z}$	κ_γ	λ_γ	$g_5^{\rm Z}$
WW	0.10	0.39	0.08	0.12
Weν	0.33	0.26	0.32	0.86
$\nu\bar{\nu}\gamma$	—	0.90	0.99	—
Combined	0.10	0.17	0.10	0.12

Table 5: Systematic errors in the determination of the TGCs $g_1^{\rm Z}$, κ_γ, λ_γ and $g_5^{\rm Z}$ for the individual processes and their combination. For each TGC, the other three are set to their SM values and the constraints $\Delta\kappa_{\rm Z} = \Delta g_1^{\rm Z} - \Delta\kappa_\gamma \tan^2\theta_w$ and $\lambda_{\rm Z} = \lambda_\gamma$ are imposed.

Process	$g_1^{\rm Z}$	κ_γ	λ_γ	$\kappa_{\rm Z}$	$\lambda_{\rm Z}$
WW	0.09	0.46	0.10	0.25	0.10
Weν	0.35	0.32	0.50	0.50	0.63
$\nu\bar{\nu}\gamma$	—	0.90	0.99	—	—
Combined	0.10	0.28	0.10	0.23	0.11

Table 6: Systematic errors in the determination of the TGCs $g_1^{\rm Z}$, κ_γ, λ_γ, $\kappa_{\rm Z}$ and $\lambda_{\rm Z}$ for the individual processes and their combination. For each TGC, all other TGCs, including $g_5^{\rm Z}$, are set to their SM values.

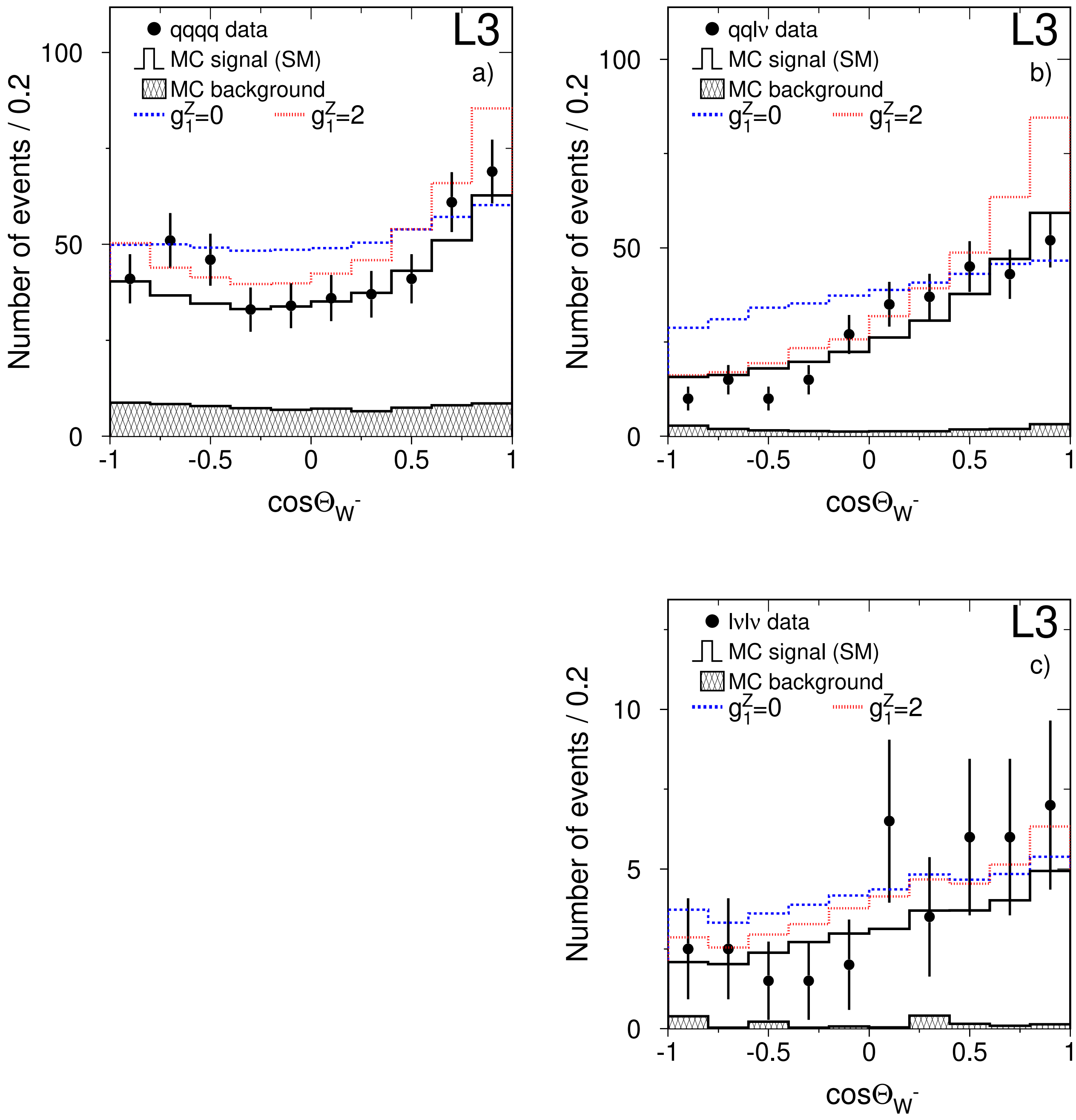

Figure 1: Distributions of the reconstructed polar scattering angle, $\cos\Theta_{\mathrm{W}}$, of the W^- boson in W-pair events for a) $qqqq$, b) $qq\ell\nu$, c) $\ell\nu\ell\nu$ events. The data collected at $\sqrt{s} = 183$ GeV are shown, together with the expectations for the SM ($g_1^{\mathrm{Z}} = 1$), and for anomalous TGCs ($g_1^{\mathrm{Z}} = 0$ or 2). For $\ell\nu\ell\nu$ events, both solutions enter with a weight of 0.5.

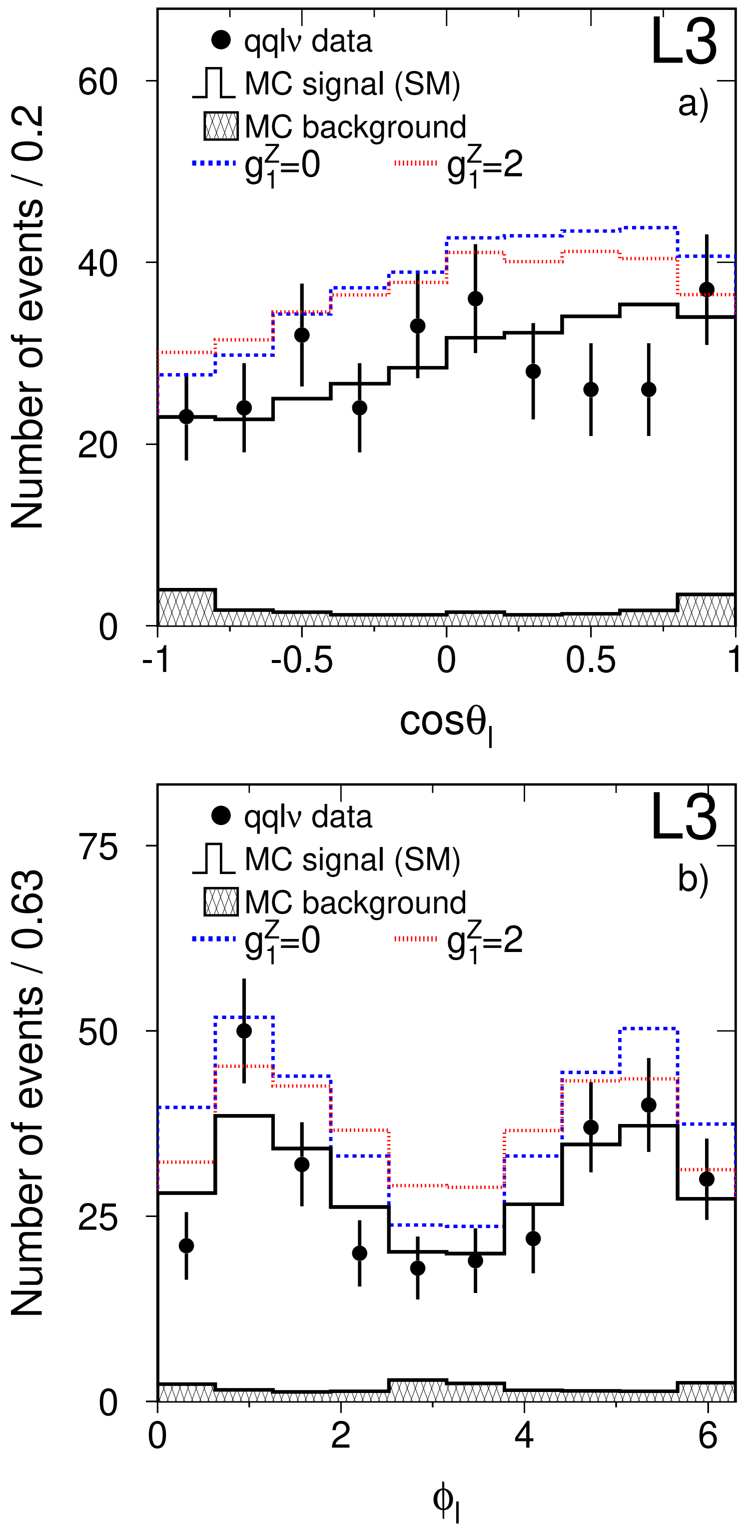

Figure 2: Distributions of the reconstructed W decay angles in $qq\ell\nu$ W-pair events, a) $\cos\theta_\ell$ and b) ϕ_ℓ. The data collected at $\sqrt{s} = 183$ GeV are shown, together with the expectations for the SM ($g_1^Z = 1$), and for anomalous TGCs, ($g_1^Z = 0$ or 2). The ϕ_ℓ distribution for W$^-$ decays is shifted by π in order to have the same ϕ_ℓ distribution for W$^-$ and W$^+$ decays.

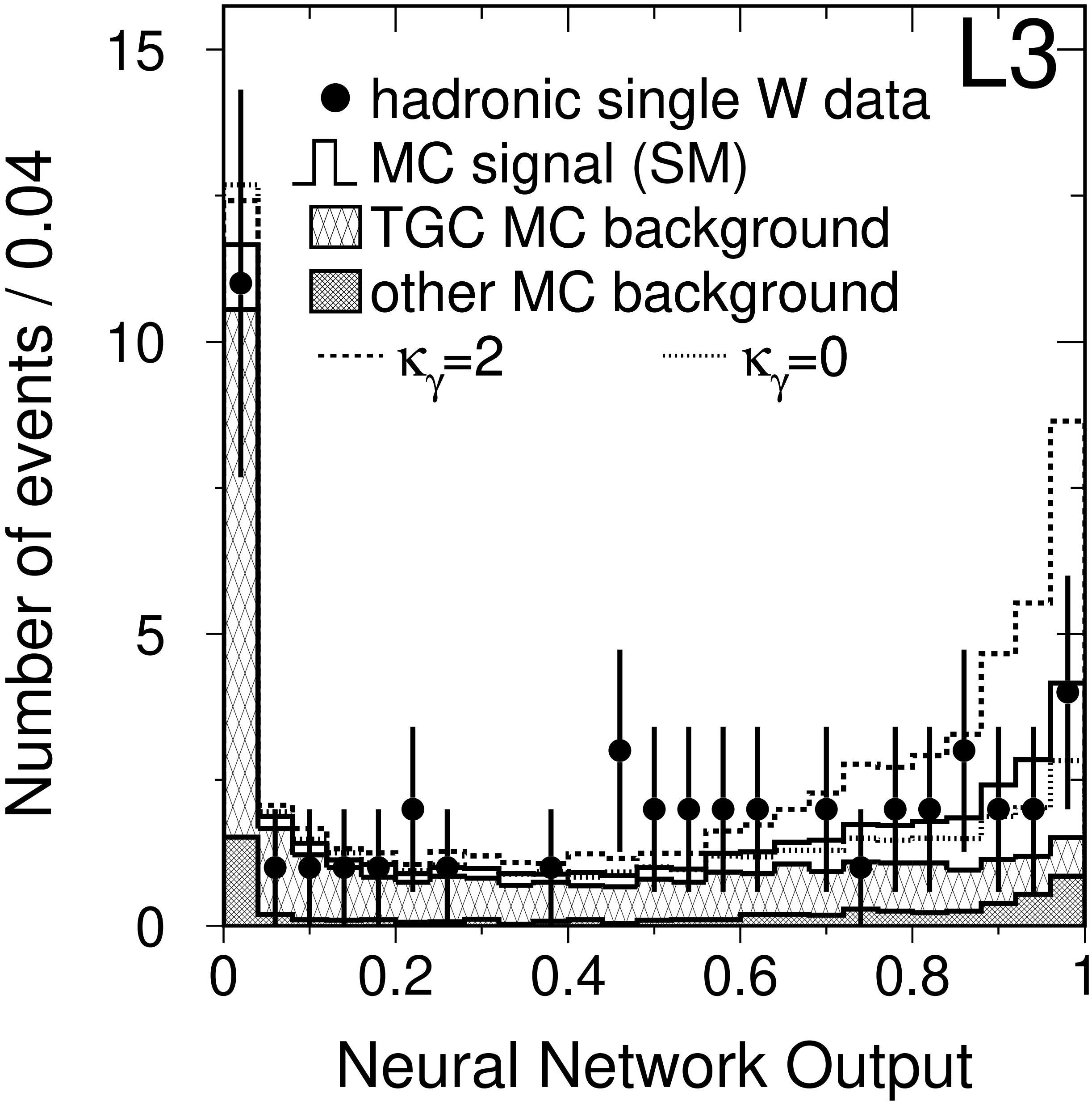

Figure 3: Distribution of the output of the neural network used in the selection of hadronic single-W events. The data collected at $\sqrt{s} = 183$ GeV are shown, together with the expectations for the SM ($\kappa_\gamma = 1$), and for anomalous TGCs ($\kappa_\gamma = 0$ or 2). The background expectation is separated into TGC-dependent W-pair background and other background independent of TGCs.

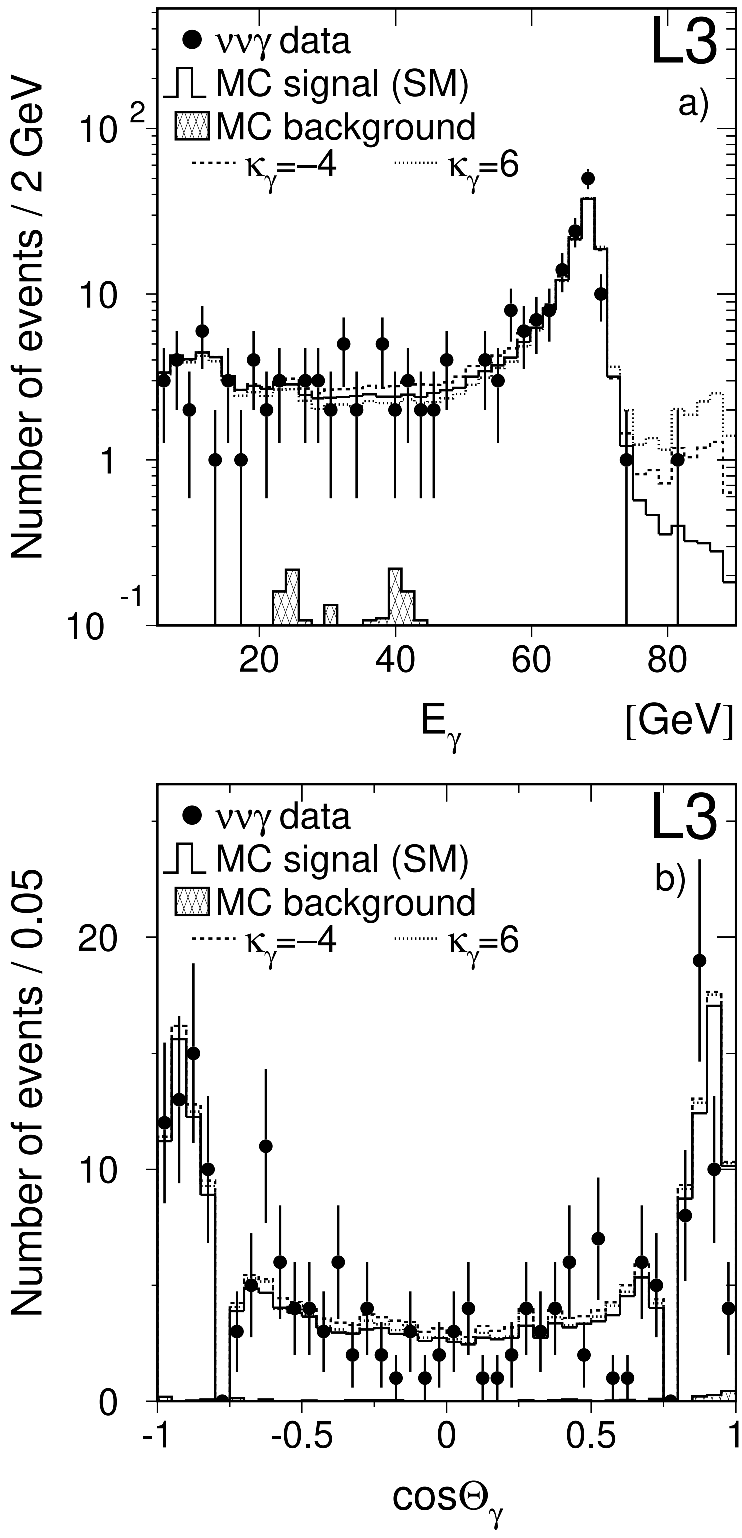

Figure 4: Distributions of a) the energy, E_γ, and b) the polar angle, Θ_γ, of the photon in single-photon events. The data collected at $\sqrt{s} = 183$ GeV are shown, together with the expectations for the SM ($\kappa_\gamma = 1$), and for anomalous TGCs ($\kappa_\gamma = -4$ or 6). The main sensitivity of single-photon events to TGCs occurs at large photon energies.

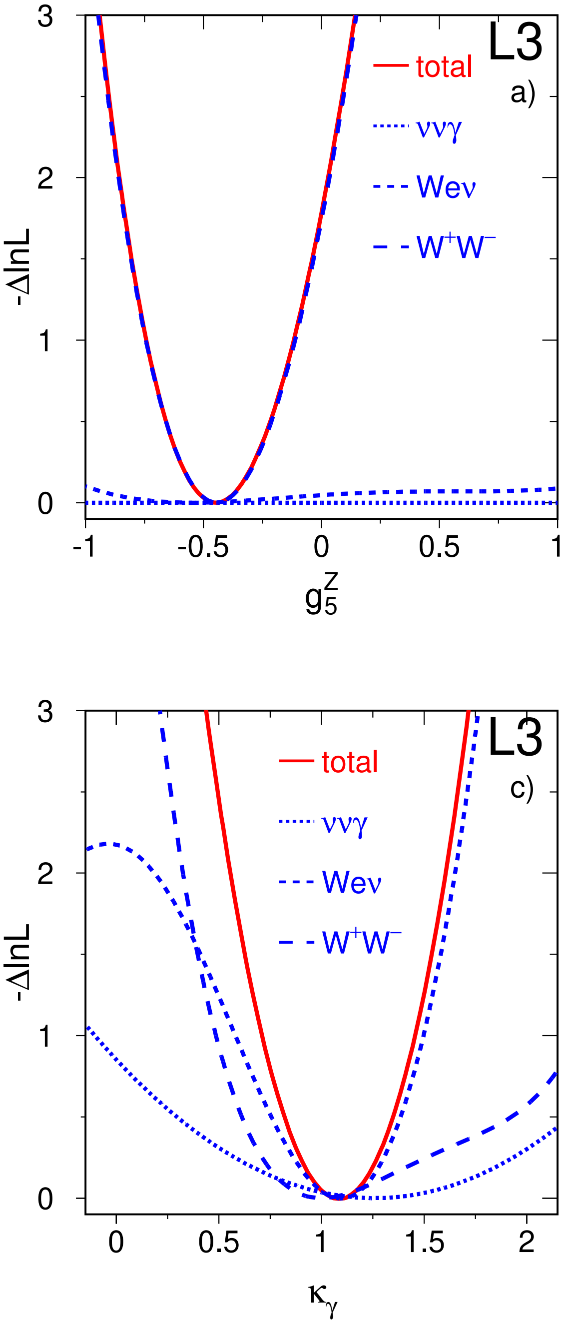

Figure 5: Negative log-likelihood functions (statistical errors only) for one-parameter fits to the TGCs a) g_5^Z, b) g_1^Z, c) κ_γ and d) λ_γ. The constraints $\Delta\kappa_Z = \Delta g_1^Z - \Delta\kappa_\gamma \tan^2\theta_w$ and $\lambda_Z = \lambda_\gamma$ are imposed.

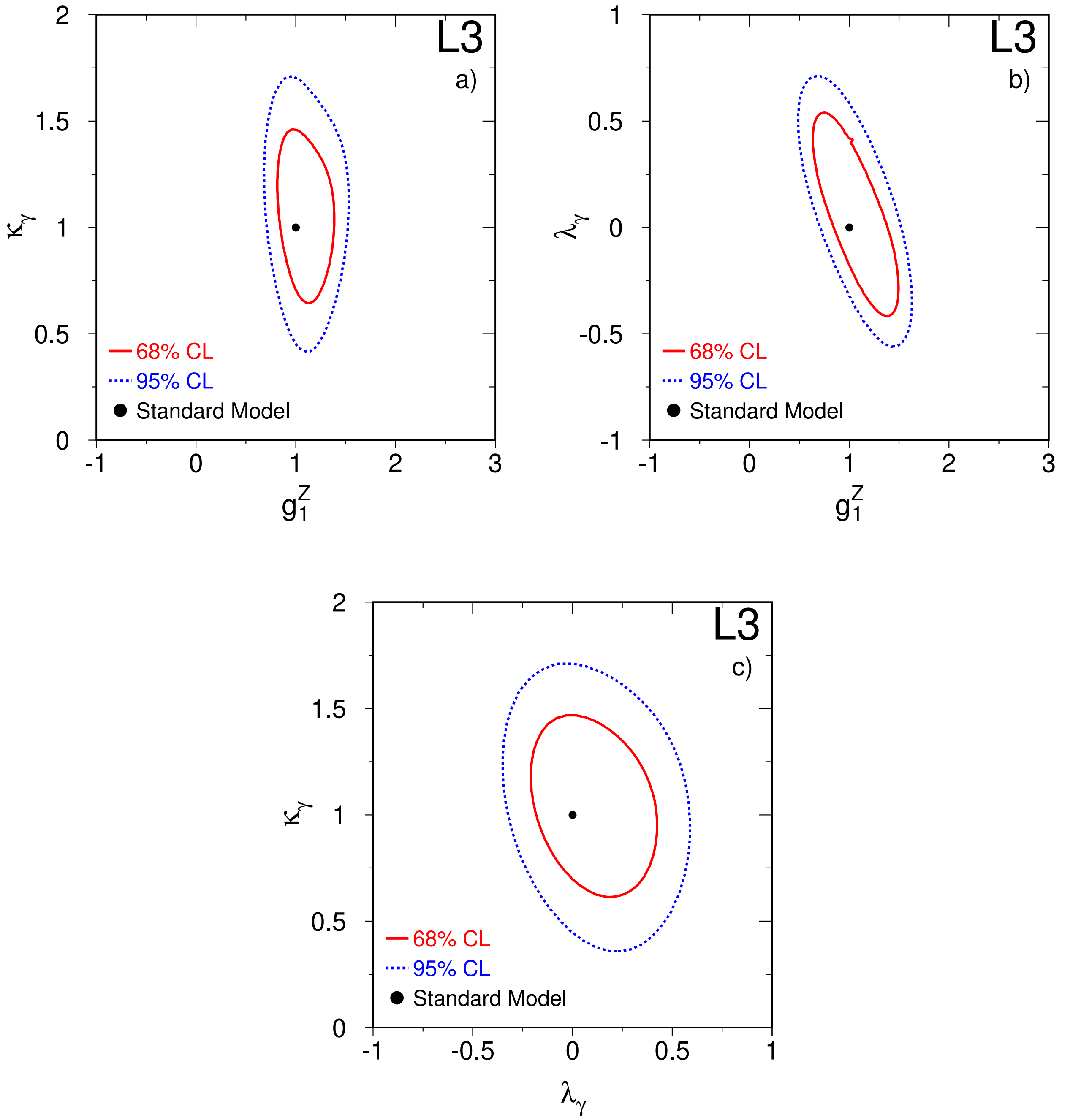

Figure 6: Contour curves of 68% and 95% probability for the two-parameter fits to the TGCs a) g_1^Z and κ_γ with $\lambda_\gamma = 0$, b) g_1^Z and λ_γ with $\kappa_\gamma = 1$, c) κ_γ and λ_γ with $g_1^Z = 1$. The constraints $g_5^Z = 0$, $\Delta\kappa_Z = \Delta g_1^Z - \Delta\kappa_\gamma \tan^2\theta_w$ and $\lambda_Z = \lambda_\gamma$ are imposed.